



# Performance of seawater-mixed concrete in the tidal environment

Tarek Uddin Mohammed\*, Hidenori Hamada, Toru Yamaji

*Materials Division, Independent Administrative Institution, Port and Airport Research Institute, 3-1-1 Nagase, Yokosuka 239-0826, Japan*

Received 18 September 2001; accepted 22 September 2003

## Abstract

Compressive strength, mineralogy, chloride ingress, and corrosion of steel bars embedded in concrete made with seawater and tap water are summarized here based on the several long-term exposure investigations under tidal environment. Seawater-mixed concrete shows earlier strength gain. After 20 years of exposure, no significant difference in the compressive strength of concrete is observed for concrete mixed with seawater and tap water. The initial amount of chloride (due to the use of seawater) may cause the initiation of corrosion at the locations of the steel bars having voids/gaps at the steel–concrete interface immediately after casting concrete. The use of seawater results in the formation of deeper corrosion pits compared to the same with tap water.

© 2004 Elsevier Ltd. All rights reserved.

**Keywords:** Compressive strength; Concrete; Corrosion; Seawater

## 1. Introduction

The discussions on the performance of seawater-mixed concrete are still reported in the recent technical literatures [1]. Generally, it is said that seawater-mixed concrete should be avoided to use in reinforced-concrete structures. In the case of unavoidable situation, the use of seawater is recommended for plain concrete [2]. We also performed several investigations on concrete mixed with seawater, tap water, and salt water. Various cements were used in these investigations, such as ordinary portland cement, blended slag and fly ash cements, moderate-heat portland cement, and high early-strength portland cement. The specimens were exposed to a tidal pool utilizing seawater directly from the sea. A summary of these investigations is reported here. The results will be very useful to understand the long-term performance of concrete mixed with tap water and seawater under the tidal environment.

## 2. Experimental methods

Two series of investigations were carried out. The concrete specimens were mixed with tap water and seawater.

The physical properties and chemical compositions of seawater are shown in Table 1. In the first series (denoted as Series 1), the cement types were ordinary portland cement, slag cement, and fly ash cements. In this series, both uncracked (cylinder specimens with a diameter of 150 mm and height of 300 mm) and cracked (prism specimens of size 100×100×600 mm) concrete specimens were investigated. Three round steel bars of diameter 9 mm were embedded at 20, 40, and 70 mm of cover depths in cylindrical specimens. Plain cylindrical concrete specimens were also made. In prism specimens, a round steel bar, 9 mm in diameter and 500 mm in length, was embedded at the middle of the section. Before exposure, a bending crack was made at the center of the prism specimen. The investigations on this series were carried out at the age of 28 days and 15 years. In the second series (denoted as Series 2), the cement types were ordinary portland cement, high early-strength portland cement, moderate-heat portland cement, and blast furnace slag cement. In this series, plain and reinforced cylindrical specimens, 150 mm in diameter and 300 mm in height, were investigated. Reinforcements were embedded at 20, 40, and 70 mm of cover depths. The investigations were carried out at 28 days at 1, 5, and 20 years of exposure. The specimens were exposed in a tidal pool created by automatic pumping into and draining out of seawater directly from the sea.

Compressive strength of concrete, chloride contents, and corrosion of steel bars in cracked and uncracked concrete

\* Corresponding author. Tel.: +81-468-44-5061; fax: +81-468-44-0255.

E-mail address: [tarek@pari.go.jp](mailto:tarek@pari.go.jp) (T.U. Mohammed).

Table 1  
Physical properties and chemical composition of seawater

Specific gravity	pH	Na (ppm)	K (ppm)	Ca (ppm)	Mg (ppm)	Cl (ppm)	SO <sub>4</sub> (ppm)	CO <sub>3</sub> (ppm)
1.022	7.77	9290	346	356	1167	17087	2378	110

were evaluated. In some cases, the mineralogy of the concrete samples was also evaluated by X-ray diffraction (XRD). Further detail of the experimental setup of these investigations can be obtained in Refs. [3–5].

A detailed experimental investigation was also carried out in the laboratory to clarify the formation of corrosion cells over the steel bars in concrete due to the presence of gap/void at the steel–concrete interface. In this case, the specimens (length 100 mm, width 230 mm, and height 290 mm) were made with 10 kg/m<sup>3</sup> NaCl in concrete to accelerate the corrosion process. Macrocell corrosion process as well as the degree of microcell corrosion of steel bars depending on their orientation in concrete was examined. For this, a specially fabricated steel bar was embedded in concrete, separating horizontal and vertical steel bars. Also, each horizontal steel bars was divided into top and bottom halves. Electrical connections among the steel bars were provided from outside of the specimens. After casting, the specimens were exposed in a closed container with constant humidity and temperature. Further detail of this experimental setup is provided later. More detail experimental setup and the process of evaluation of macro- and microcell corrosion can be obtained in Ref. [6].

### 3. Experimental results and discussion

The results are reported in two separate sections entitled as “Concrete Mixed with Seawater and Tap Water” (Section 3.1) and “Concrete Mixed with Salt Water” (Section 3.2). In Section 3.1, the results related to the 15- and 20-year-old specimens (Series 1 and 2, respectively) are discussed. In Section 3.2, the corrosion of steel bars in concrete with the presence of void at the steel–concrete interface is summarized and correlated with the corrosion of steel bars in seawater-mixed concrete.

#### 3.1. Concrete mixed with seawater and tap water

##### 3.1.1. Compressive strength—Series 1

Compressive strengths of cylinder specimens at the age of 28 days and 15 years of exposure to the tidal environment are shown in Fig. 1. Here OPC, SCA, SCB, SCC, and FACB mean ordinary portland cement, slag cement of Type A, slag cement of Type B, slag cement of Type C, and fly ash cement of Type B, respectively. In SCA, SCB, and SCC, the slag contents are 5–30%, 30–60%, and 60–70% of the cement mass, respectively. In FACB, the fly ash content is 10–20% of cement mass. Further specifications on the blended cements can be obtained in JIS R5211-1992 and

JIS R5213-1992. The symbols T, S, and numbers (Fig. 1) represent tap water, seawater, and water-to-cement ratio, respectively. The mixture proportions and cement compositions can be obtained in Ref. [3]. The use of seawater causes an earlier strength gain compared to the same with tap water. It is understood that at the early age, the microstructure of concrete improved due to the use of seawater. It is expected due to the acceleration of hydration process with the presence of chloride. The use of seawater does not cause the deterioration of concrete strength after 15 years of exposure in a tidal pool. The interim strength of concrete between 28 days and 15 years of exposure cannot be judged from this experimental series.

##### 3.1.2. Compressive strength and mineralogy—Series 2

Compressive strength of cylinder specimens at the age of 28 days and 1, 5, and 20 years of exposure in a tidal pool are shown in Fig. 2 for Series 2. In this series, ordinary portland cement (OPC1 and OPC2), high early-strength portland cement (HESPC), moderate-heat portland cement (MHPC), and slag cement of Type B (SCB1 and SCB2) were investigated. In OPC1 and OPC2, the sulfate contents are 2.0% and 3.9%, respectively. In SCB1 and SCB2, the sulfate contents are 2.4% and 4.3%, respectively. The detail of mixture proportions and cement compositions of this series can be obtained in Ref. [5]. A gain in compressive strength of concrete is observed until the age of 5 years. Then it reduces gradually until the age of 10 years, and at the age of 20 years, becomes the same or less than the 28-day strength of concrete. The same variation in strength with the exposure age was also observed for concrete mixed with tap water. The exact reason for this strength variation cannot be explained as the detail analysis on the gradual change in the microstructure and mineralogy of concrete was not carried out. Probable reasons of strength gain at the early stage (28 days to 5 years) of exposure are the ongoing hydration of cement in concrete, and the deposition of ettringite and Friedel’s salt in the air voids in concrete caused by the diffused sulfate and chloride. From 10 to 20 years, no significant reduction in strength is observed. The stability in strength after 10 years is expected due to the improvement of the microstructures at the outer region of the specimens caused by the deposition of ettringite as well as Friedel’s salt. The improvement of microstructure at the outer region of the specimens after 15 years of exposure is reported in Ref. [7]. The improved microstructure at the outer region causes to screen the diffused ions from seawater into concrete at the outer region. Further research on the gradual change in microstructure of concrete is still necessary to confirm the

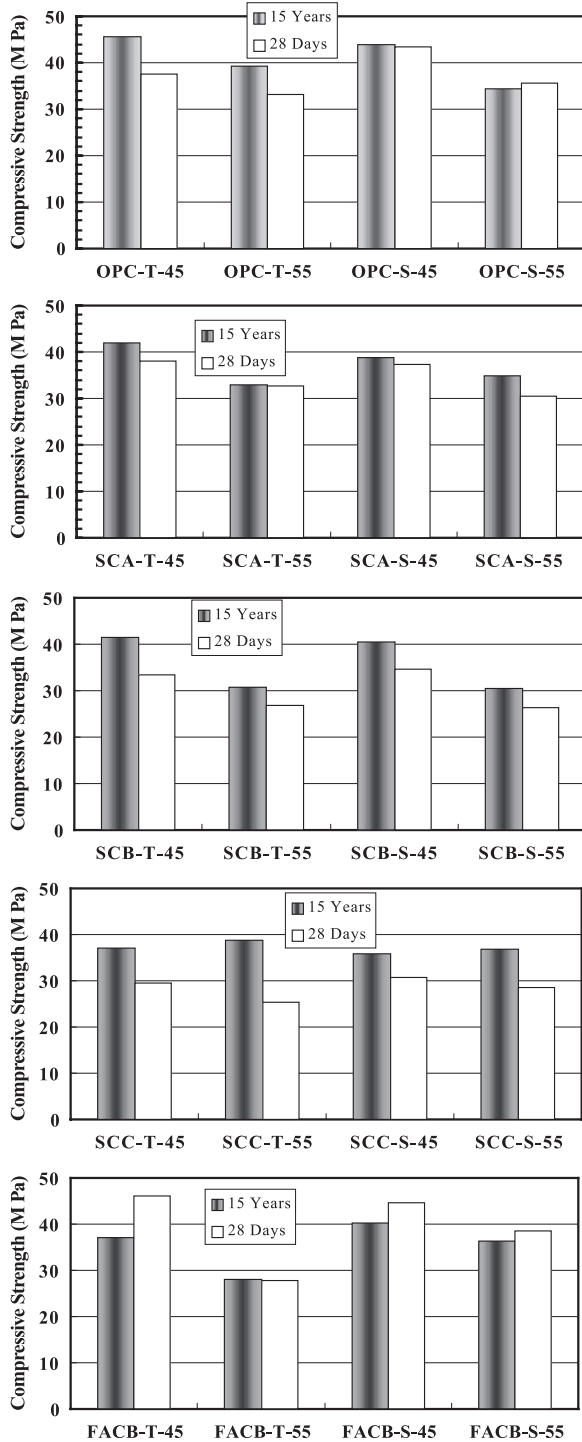


Fig. 1. Compressive strength of concrete mixed with seawater and tap water.

exact mechanism related to the strength gain at the early stage, strength reduction at the intermediate stage, and the stability of strength at the later stage of exposure as observed in Fig. 2. The mineralogical composition of concrete after 20 years of exposure is explained later. It

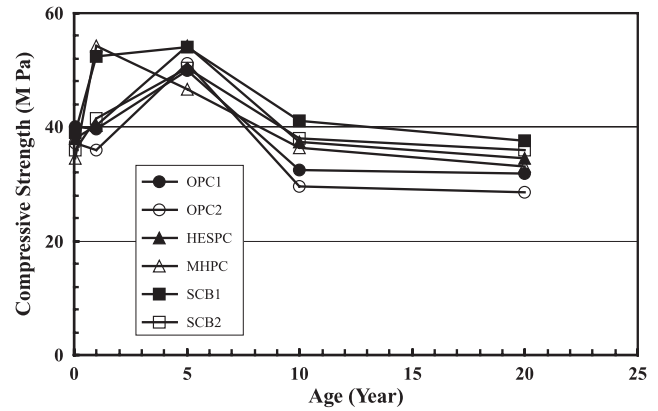


Fig. 2. Compressive strength of concrete mixed with seawater at the different ages of exposure.

is worth to mention that in Series 1, the tests was conducted at the age of 28 days and 15 years of exposure, therefore, the strength at the interim period between 28 days and 15 years cannot be judged as in Series 2.

Compressive strength ratios (seawater-mixed concrete divided by tap water-mixed concrete) are shown in Fig. 3 for Series 2. It is clear that the use of seawater causes an earlier strength gain. However, after a long exposure period, no significant variation is observed. It is understood that after a long-term of exposure, the compressive strength of concrete is independent of the type of mixing water, such as tap water and seawater.

The results of XRD analysis of concrete after 20 years of exposure are listed in Table 2. The type of cement and mixing water do not influence the contents of ettringite in concrete. Friedel's salt is observed in all samples. However, it is not observed at the center of the specimens, especially for slag cements. Calcium carbonate (generated from the reaction of calcium hydroxide with dissolved carbon dioxide in seawater) is recognized in all cases. There is no sign of indication that the seawater-mixed concrete is less durable than the tap water-mixed concrete.

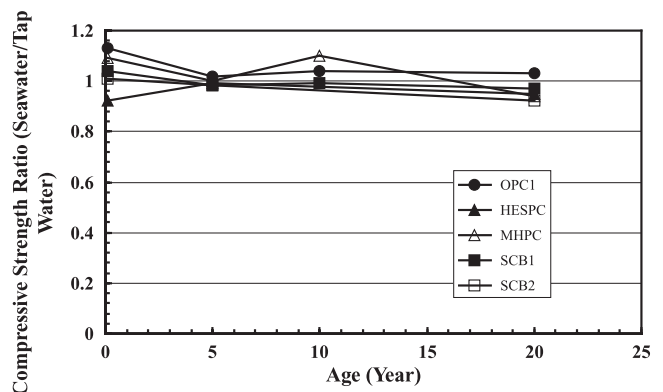


Fig. 3. Compressive strength ratio at the different ages of exposure (seawater case/tap water case).

Table 2  
Results of XRD analysis

Specimen	Depth of sampling (cm)	Ettringite	Friedel's salt	CaCO <sub>3</sub>
OPC1-T-53	1	+	++	+
	3	+	++	+
	5	+	++	+
	7.5	+	++	+
OPC1-S-53	1	+	++	+
	7.5	+	++	+
OPC2-T-55	1	+	++	+
	7.5	+	++	+
OPC2-S-55	1	+	++	+
	7.5	+	++	+
HESPC-T-53	1	+	++	+
	7.5	+	++	++
HESPC-S-55	1	+	++	+
	7.5	+	++	+
MHPC-T-52	1	+	++	+
	7.5	+	+	+
MHPC-S-53	1	+	++	+
	7.5	+	++	+
SCB1-T-52	1	+	++	+
	3	+	+	++
	5	+	+	+
	7.5	+	+	+
SCB1-S-53	1	+	++	+
	7.5	+	+	+
SCB2-T-55	1	+	++	+
	7.5	+	+	+
SCB2-S-56	1	+	+	+
	7.5	+	+	+

+ = less than 500 counts per second; ++ = 500–2000 counts per second; OPC1 and OPC2 = ordinary portland cement; HESPC = high early-strength portland cement; MHPC = moderate-heat portland cement; SCB1 and SCB2 = blast furnace portland cement of Type B; T and S = type of mixing water, T for tap water and S for seawater. The number in the title of each specimen represents the water-to-cement ratio.

### 3.1.3. Chloride diffusion in concrete—Series 1

Acid-soluble chloride concentrations in concrete mixed with seawater and tap water are shown in Fig. 4. It is found that concrete mixed with seawater has more chloride concentrations than the concrete mixed with tap water irrespective of the cement types, such as OPC, SCA, SCB, SCC, and FACB, due to the initial amount of chloride in concrete from seawater. The diffused amount of chloride in concrete was calculated by subtracting the initial amount of chloride in concrete from the total amount of chloride estimated after 15 years of exposure. The initial amount of chloride in concrete were estimated at 0.95% and 0.75% of cement mass for W/C=0.55 and 0.45, respectively, based on the chloride content in seawater and cement and water content in the mixture proportions of concrete. The diffused amount of chloride in concrete made with seawater is plotted in Fig. 5 against the total amount of chloride content in concrete mixed with tap water. For W/C=0.45, it is found that the deviation of the data from the line of equity is low. On the other hand, for W/C=0.55, the diffused amount of chloride for concrete mixed with seawater is lower than the total amount of chloride concentration for concrete made with tap

water. The results suggest that the diffusion coefficient of chloride in concrete with W/C=0.55 is improved due to the use of seawater as mixing water. However, it does not result in the reduction of total chloride concentration (compared with W/C=0.45) in concrete after 15 years of exposure. Unfortunately, the microstructure of concrete made with tap water and seawater was not checked for further clarification. However, it is expected that the use of seawater may improve the diffusion coefficient due to the precipitation

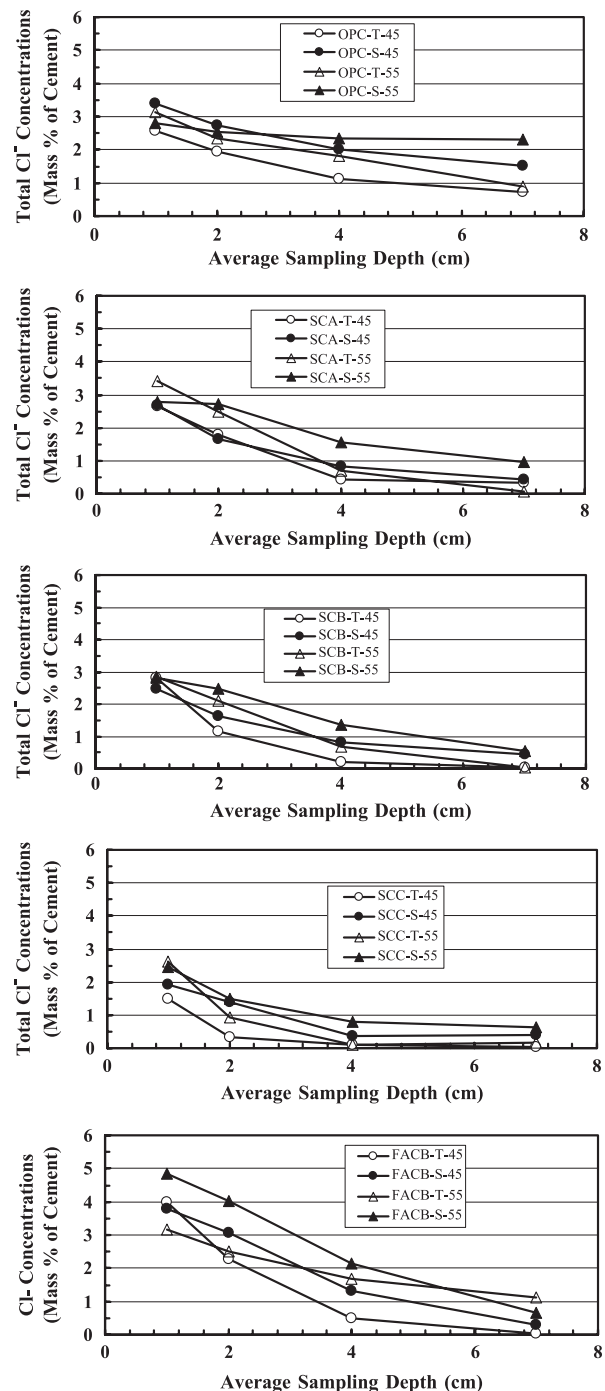


Fig. 4. Chloride ion profiles in concrete made with seawater and tap water (after 15 years exposure in tidal environment).

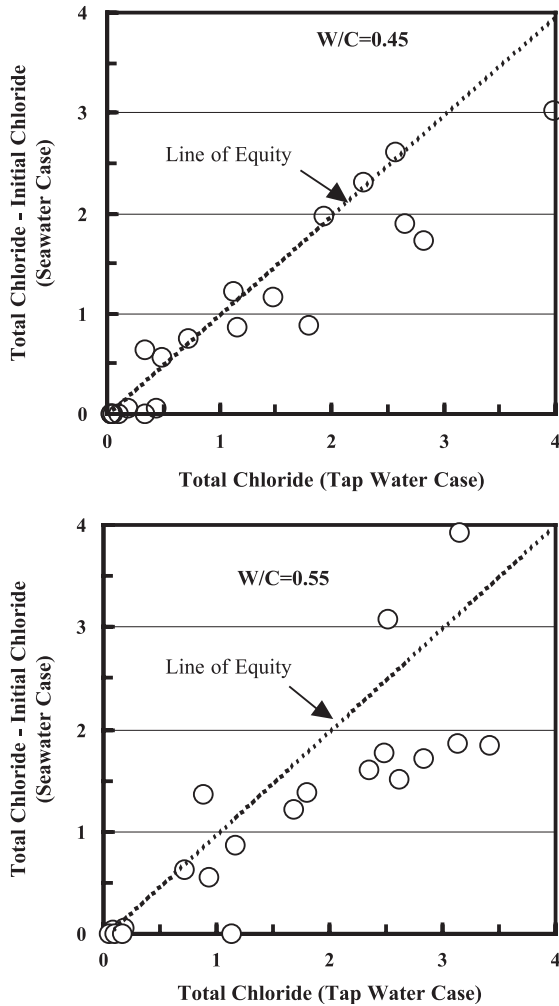


Fig. 5. Chloride diffusion in concrete mixed with seawater and tap water (after 15 years of exposure in the tidal environment).

of calcium chloroaluminate compound (Friedel's salt) as well as the more ettringite in the pore system. The influence is found to be significant for higher W/C.

Based on the abovementioned results, the total amount of chloride concentrations, and the progress of corrosion of steel bars in concrete with time are schematically represented in Fig. 6 for concrete mixed with tap water and seawater (especially for concrete with low water-to-cement ratio, such as W/C=0.45, i.e., assuming the same diffusion coefficient for tap water- and seawater-mixed concrete). It is assumed that corrosion of steel bars in concrete will be started at a particular time when the amount of chloride concentration over the steel bar reaches or exceeds the chloride threshold level. For tap water case, the time to initiate corrosion is defined as  $t_{t-tw}$ . The same for concrete mixed with seawater is  $t_{t-sw}$  without any consideration of voids at the steel–concrete interface. Therefore, the initiation time of corrosion due to the use of seawater will be earlier by a time period  $\Delta t = (t_{t-tw} - t_{t-sw})$  compared with the same in concrete made with tap water. Based on the observations on the corrosion of steel bars in concrete, it was observed that the presence of voids/

gaps at the steel concrete interface causes the formation of corrosion pits. The size of voids can be varied from 100  $\mu\text{m}$  to several millimeters. If there is a void at the steel–concrete interface, the corrosion process may continue immediately after placing concrete mixed with seawater or brackish water. In such a situation, it can be judged that the initiation of corrosion will be started at time  $t=0$  (realistic consideration or consideration of voids at the steel–concrete interface). Therefore, the term  $t_{t-sw}$  will become zero and finally  $\Delta t = t_{t-tw}$ . The value of  $t_{t-tw}$  can be considered as a two-digit figure in years based on the properties of concrete and the location of steel bars in concrete. Of course, this figure will influence the long-term durability of concrete structures. After initiation of corrosion, the higher amount of chloride in concrete mixed with seawater will also accelerate the corrosion rate and finally will create deep corrosion pits earlier. It will result in earlier repair works as schematically explained in Fig. 6.

In addition to the uncracked concrete, cracked concrete specimens of size 100×100×600 mm made with seawater and tap water were also investigated. Water soluble chloride concentration in concrete at the cracked region for concrete mixed with seawater and tap water are summarized in Table 3. A tendency of having more chloride at the cracked region is observed for concrete mixed with seawater than the same with tap water. It is important to note that in this investiga-

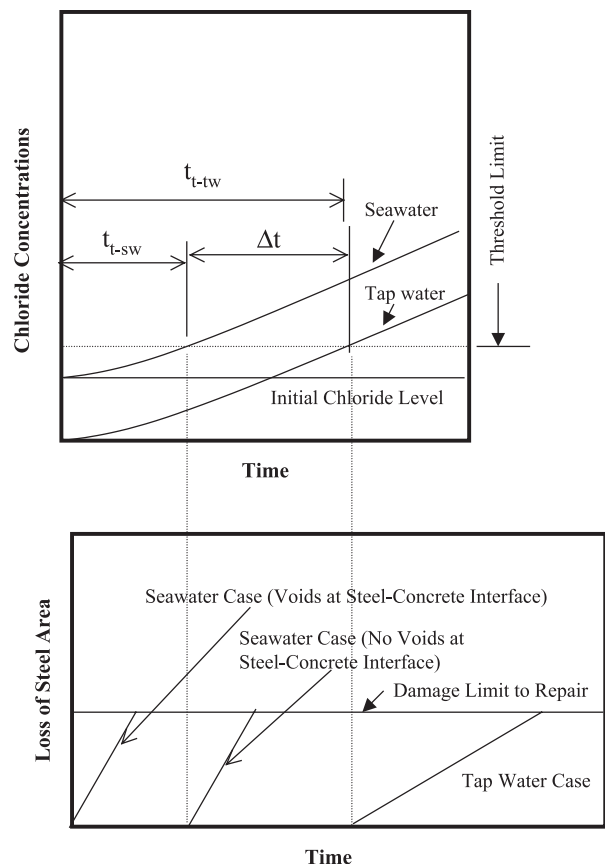


Fig. 6. Schematic diagrams—initiation of corrosion (top) and progress of corrosion (bottom).



Table 3  
Water soluble chloride concentrations in concrete at the cracked region

Specimens	Crack widths (mm)			Chloride concentrations (mass% of cement)		
	(1)	(2)	(3)	(1)	(2)	(3)
OPC-T-45	0.2	0.1	0.1	1.28	1.14	1.38
OPC-T-55	0.1	0.1	0.1	1.48	1.78	1.58
OPC-S-45	0.1	2.0	0.1	1.35	2.24	1.85
OPC-S-55	0.1	0.1	0.1	1.90	2.0	1.70
SCB-T-45	0.3	0.1	5.0	0.45	0.41	3.20
SCB-S-45	0.3	0.2	0.1	1.26	0.88	0.70
FACB-T-45	0.1	0.3	0.5	0.90	0.82	1.42
FACB-S-45	0.2	0.2	0.2	1.76	1.03	0.86

OPC=ordinary portland cement; SCA=slag cement of Type A; SCB=slag cement of Type B; SCC=slag cement of Type C; FACB=ordinary portland cement. T and S=type of mixing water, T for tap water and S for seawater. The number in the title of each specimen represents the water-to-cement ratio. (1), (2), and (3) are the individual specimens of each group.

tion, most of the cracks (crack widths  $\leq 0.5$  mm) were healed during the exposure in the tidal environment for 15 years. These results are expected to explain separately in future. More results on this investigation can be obtained in Ref. [4].

#### 3.1.4. Physical evaluation of corrosion (pit numbers and depths)—Series 1

After exposure in the tidal environment for 15 years (Series 1), reinforced cylindrical concrete specimens were split opened to check the steel bars (the length of the bar was 180 mm) located at 20, 40, and 70 mm of covered concrete depths. The number of pits and pit depths over the steel bars at the different cover depths are listed in Table 4 for different

Table 4  
Pit numbers and depths over the steel bar at different concrete covers

Specimen	Number of pits at different cover depths			Pit depth (mm) at different depths		
	20 mm	40 mm	70 mm	20 mm	40 mm	70 mm
OPC-T-45	6	2	0	1.5	1	—
OPC-T-55	10	5	0	1.5	1	—
OPC-S-45	15	4	0	2	1.5	—
OPC-S-55	15	3	3	1	1	1
SCA-T-45	3	0	0	1	—	—
SCA-T-55	2	0	0	1	—	—
SCA-S-45	10	0	0	1.5	—	—
SCA-S-55	12	4	0	2	1.5	—
SCB-T-45	0	0	0	—	—	—
SCB-T-55	12	0	0	1	—	—
SCB-S-45	5	1	0	1	1	—
SCB-S-55	1	2	0	1	1	—
SCC-T-45	0	0	0	—	—	—
SCC-T-55	7	0	0	1	—	—
SCC-S-45	3	0	0	1.5	—	—
SCC-S-55	5	0	0	1	—	—
FACB-T-45	5	0	0	0.5	—	—
FACB-T-55	16	6	0	1.5	1	—
FACB-S-45	11	4	0	1	1.5	—
FACB-S-55	11	6	0	1	1	—

The symbols are explained in Table 3. Pit depths less than 0.5 mm are not counted.

mixing water and different types of cement. It is seen that the use of seawater results in higher pit numbers and deeper pit depths compared to the same with tap water. The voids at the steel–concrete interface and the presence of chloride seem to be the main reasons against the formation of corrosion pits. If concrete is mixed with seawater, the corrosion process may continue just after placing concrete. However, in the case of tap water-mixed concrete, sometime will need to penetrate the required chloride in concrete as explained with some schematic diagram before. A typical case of corrosion pit over the steel bars made with seawater is shown in Fig. 7. Formation of deeper corrosion pit is commonly observed over the steel bars in seawater-mixed concrete due to the presence of void at the steel–concrete interface.

Lee et al. [8], based on the investigation of concrete specimens after 35 years exposure in the marine environment, found that the top layer horizontal bars are more corroded due to the blocking of bleeding water under the bar after casting concrete. Yonezawa et al. [9] also concluded that the formation of voids at the steel–concrete interface is a necessary condition for active corrosion in concrete with moderate chloride content. Similar observation was also reported by Castel et al. [10] and Ohno et al. [11].

The depth of corrosion over the steel bars in cracked concrete mixed with seawater and tap water is listed in Table 5. It is already noted that during the exposure for 15 years, most of the cracks (crack width  $\leq 0.5$  mm) were healed irrespective of the mixing water and cement types. The healing is expected to cease or reduce the corrosion rate significantly. The depth of corrosion at the uncracked regions indicates that the use of seawater results in deeper corrosion pits.

#### 3.2. Concrete mixed with salt water

To explain the corrosion process of steel bars in concrete mixed with seawater, the results of another investigation are

FACB-S-45, Concrete Cover = 2 cm

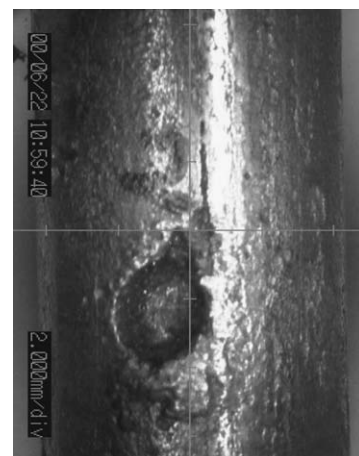


Fig. 7. Pit over the steel bar (concrete mixed with seawater).

Table 5  
Maximum pit depths at cracked and uncracked regions

Specimens	Crack width (mm)			Maximum pit depths at cracked regions (mm)			Maximum pit depths at uncracked regions (mm)		
	(1)	(2)	(3)	(1)	(2)	(3)	(1)	(2)	(3)
OPC-T-45	0.2	0.1	0.1	0.5	nil	0.5	1.0	0.5	1.5
OPC-T-55	0.1	0.1	0.1	0.5	nil	nil	2.0	1.0	1.0
OPC-S-45	0.1	2	0.1	1.0	1.0	0.5	1.0	1.5	1.5
OPC-S-55	0.1	0.1	0.1	nil	1.5	nil	0.5	1.5	1.5
SCA-T-45	0.1	0.3	0.2	nil	0.5	nil	nil	1.0	nil
SCB-T-45	0.3	0.1	5	0.5	nil	3.5 <sup>a</sup>	nil	nil	nil
SCB-S-45	0.3	0.2	0.1	nil	nil	nil	nil	nil	0.5
FACB-T-45	0.1	0.3	0.5	0.5	1.0	1.5	0.5	0.5	0.5
FACB-S-45	0.2	0.2	0.2	nil	nil	0.5	0.5	nil	0.5

The symbols and names of specimens are explained in Table 3. The specimens of each case are defined as (1), (2), and (3).

<sup>a</sup> Significant loss of area.

quoted here. In this case, 10 kg/m<sup>3</sup> of sodium chloride salt was added with the mixing water to accelerate the process of corrosion. Water-to-cement ratios were 0.5 and 0.7. Ord-

nary portland cement was used. Initial chloride contents (total) in the mixture were estimated at 1.85% and 2.6% of cement mass for W/C=0.5 and 0.7, respectively. Detail

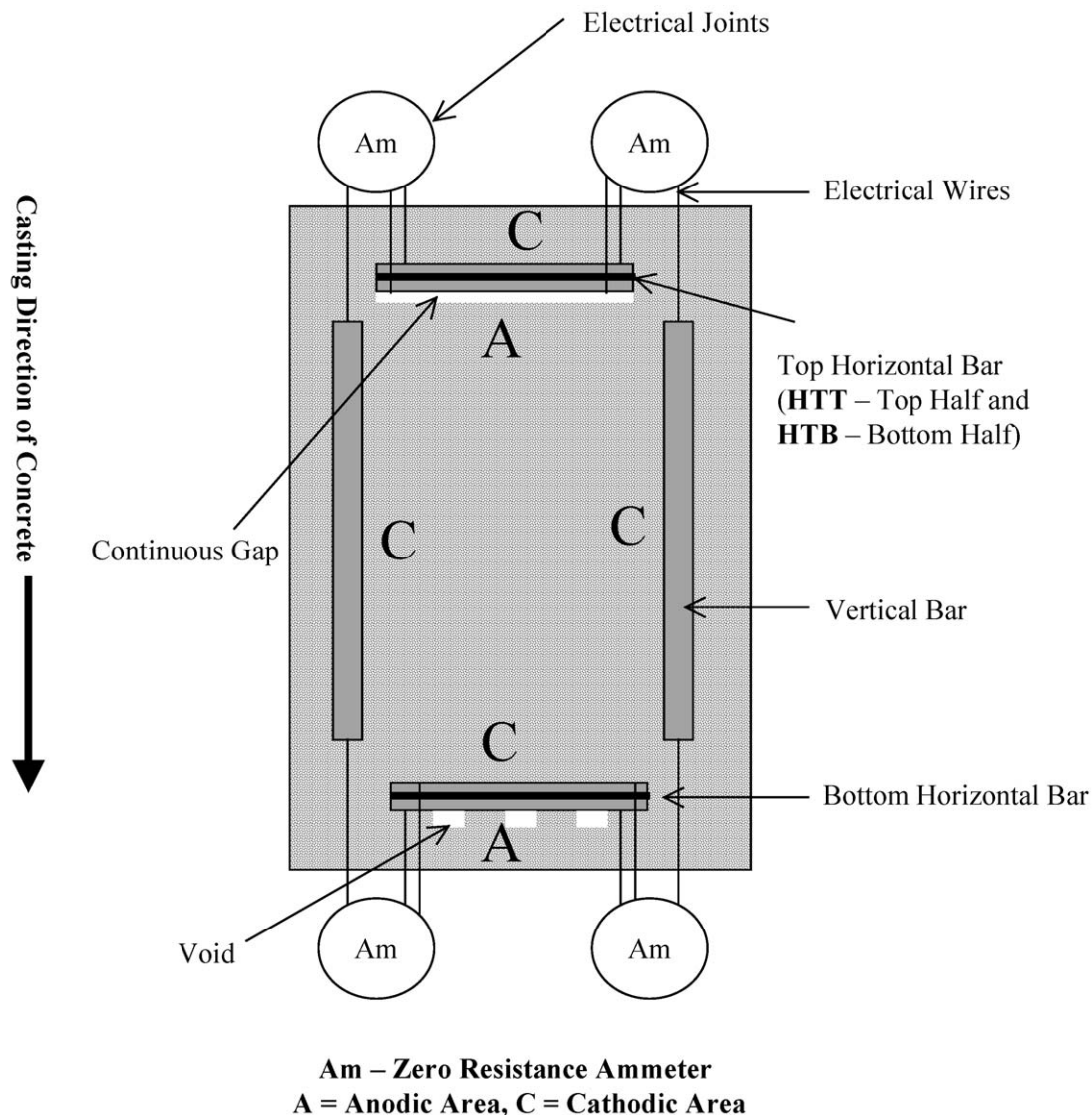


Fig. 8. Macrocell formation among the steel bars in concrete.



mixture proportion and layout of the specimens can be obtained in Ref. [6]. Based on the experimental results explained in Ref. [6], the typical process of macro corrosion cell formation is shown in Fig. 8. In this experimental setup, the horizontal steel elements divided into top and bottom halves and connected with epoxy like a sandwich. In addition, the vertical steel elements were separated from the horizontal steel bars. All steel elements were connected electrically outside the specimens to measure the flow of electrons generated by the corrosion reaction (macrocell corrosion). Based on this experimental layout, it was also able to measure polarization resistance over a specified steel element (such as top or bottom halves) by isolating it from other steel elements. The AC impedance method was applied to measure polarization resistance. Microcell corrosion current density was calculated from the polarization resistance data. Detailed experimental method can be obtained in Ref. [6].

Differential plastic settlement of concrete against the steel bars and blocking of bleeding water cause the formation of gap under the horizontal steel bar. As a result, from the viewpoint of macrocell corrosion, these portions (with gap) act as anode (denoted as A in Fig. 8) and coupled with the other steel portions (good interfacial condition with concrete), i.e., the cathodes (denoted as C). In addition, the microcell corrosion current density of the location with gap at the steel–concrete interface was also higher (such as the bottom part of the top horizontal steel bar). These locations are subjected to a significant amount of corrosion caused by the combination of macro- and microcell corrosions. The vertical steel bars and top half of horizontally oriented steel bars were not corroded at all [6].

The condition of the horizontal steel bars (top and bottom parts of the top-level horizontal steel bars) after 60 days of casting concrete is shown in Fig. 9 for  $W/C=0.5$  and  $0.7$ . The bottom half of the bar (HTB) is totally corroded due to the presence of gap under bottom half, however the top half (HTT) of the bar is not corroded at all. The macrocell corrosion process can be explained as a DC battery cell with anode (bottom part) and cathode (top part) electrically connected in an electrolytic media of concrete.

Unfortunately, the same investigation on the specimens mixed with seawater was not carried out. However, the same process of corrosion as mentioned above can be expected for the steel bars embedded in concrete mixed with seawater. Immediately after casting concrete, the corrosion process is expected to continue due to the presence of voids/gaps at the steel–concrete interface. In Ref. [12], corrosion of steel bars of 23-year-old concrete specimens exposed to tidal and atmospheric environments was reported. It was noted that the presence of gap under the steel bars caused the corrosion of steel bar although the chloride concentration was negligible (less than 0.1% of cement mass) for the atmospheric exposure environment. Further investigation on the macrocell and microcell corrosion was conducted under 3.5%

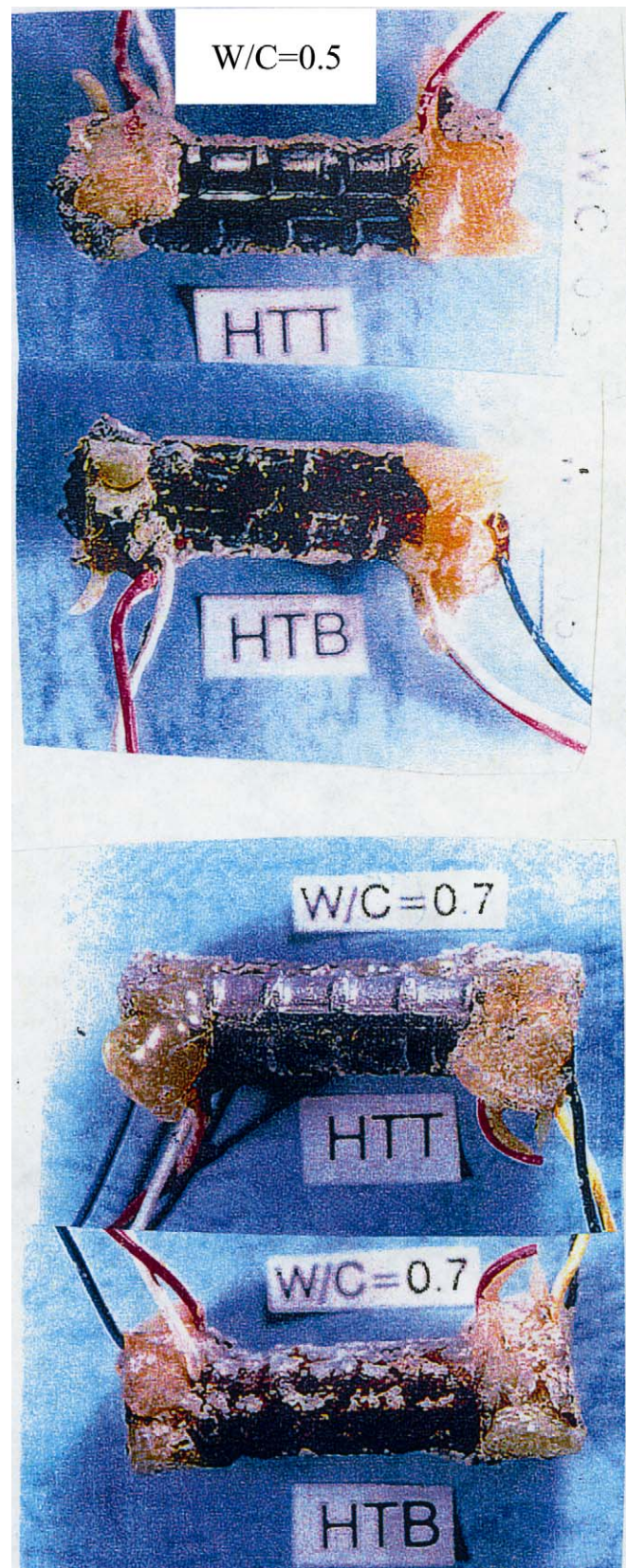


Fig. 9. Photographs of top horizontal steel portions (top pair:  $W/C=0.5$ , bottom pair:  $W/C=0.7$ ).



saltwater spray environment. The results were reported in Ref. [13].

#### 4. Conclusions

The following conclusions are drawn based on the scope of this article:

- Seawater-mixed concrete shows earlier strength gain compared to the tap water-mixed concrete. However, after a long-term of exposure, no significant difference in compressive strength is observed.
- The initial amount of chloride (due to the use of seawater) may cause the initiation of corrosion at the locations of the steel bars having voids/gaps at the steel–concrete interface immediately after casting concrete.
- The use of seawater results in the formation of deeper corrosion pits compared to the same with tap water.

#### References

- [1] A. Neville, Seawater in the mixture, *Concr. Int.*, (January 2001) 48–51.
- [2] Standard Specification for Design and Construction of Concrete Structures, Part 2 (Construction), 1st ed., Japan Society of Civil Engineers, Tokyo, Japan, 1986 (SP-2).
- [3] T.U. Mohammed, T. Yamaji, A. Toshiyuki, H. Hamada, Marine durability of 15-year old concrete specimens made with ordinary Portland, slag and fly ash cement, *ACI Spec. Publ.* 199-30 2 (2001) 541–560.
- [4] T.U. Mohammed, T. Yamaji, A. Toshiyuki, H. Hamada, Corrosion of steel bars in cracked concrete made with ordinary Portland, slag and fly ash cements, *ACI Spec. Publ.* 199-40 2 (2001) 699–718.
- [5] T. Fukute, H. Hamada, A study on the durability of concrete exposed in the marine environment for 20 years, *Rep. Port Harb. Res. Inst.* 31 (5) (1993) 251–272.
- [6] T.U. Mohammed, N. Otsuki, M. Hisada, Corrosion of steel bars with respect to orientation in concrete, *ACI Mater. J.* 96 (2) (1999) 154–159.
- [7] T.U. Mohammed, T. Yamaji, H. Hamada, Chloride diffusion, microstructures and mineralogy of concrete after 15 years of exposure in the tidal environment, *ACI Mater. J.* 99 (3) (2002) 256–263.
- [8] S.K. Lee, D.V. Reddy, W.H. Hartt, M. Arockiasamy, E.F. O’Neil, Marine concrete durability—condition survey of certain tensile crack exposure beams at treat island, Maine, USA, *ACI Spec. Publ.* 145, (1994) 371–388.
- [9] T. Yonezawa, V. Ashworth, R.P.M. Procter, Pore solution composition and chloride effects on the corrosion of steel in concrete, *Corros. Eng.* 44 (7) (July 1988) 489–499.
- [10] A. Castel, R. Francois, G. Arliguie, Factors other than chloride level influencing corrosion rate of reinforcement, *ACI Spec. Publ.* 192, (2000) 629–644.
- [11] Y. Ohno, K. Suzuki, S. Praparntanatorn, Macrocell corrosion of steel in uncracked concrete, in: R.N. Swamy (Ed.), *Corrosion and Corrosion Protection of Steel in Concrete*, International Conference, July 24–29. Sheffield Academic Press, Sheffield, UK, 1994, pp. 224–235.
- [12] T.U. Mohammed, N. Otsuki, M. Hisada, H. Hamada, Marine durability of 23-year old reinforced concrete beams, *ACI Spec. Publ.* 192-65, (2000) 1071–1088.
- [13] T.U. Mohammed, N. Otsuki, H. Hamada, Y. Toru, Chloride-induced corrosion of steel bars in concrete with the presence of gap at the steel–concrete interface, *ACI Mater. J.* 99 (2) (2002) 149–156.